The Company of **Biologists**

RESEARCH ARTICLE

UPF2, a nonsense-mediated mRNA decay factor, is required for prepubertal Sertoli cell development and male fertility by ensuring fidelity of the transcriptome

Jianqiang Bao[1,*,‡], Chong Tang[1], Shuiqiao Yuan[1], Bo T. Porse[2,3,4] and Wei Yan[1,‡]

ABSTRACT

Nonsense-mediated mRNA decay (NMD) represents a highly conserved RNA surveillance mechanism through which mRNA transcripts bearing premature termination codons (PTCs) are selectively degraded to maintain transcriptomic fidelity in the cell. Numerous *in vitro* studies have demonstrated the importance of the NMD pathway; however, evidence supporting its physiological necessity has only just started to emerge. Here, we report that ablation of *Upf2*, which encodes a core NMD factor, in murine embryonic Sertoli cells (SCs) leads to severe testicular atrophy and male sterility owing to rapid depletion of both SCs and germ cells during prepubertal testicular development. RNA-Seq and bioinformatic analyses revealed impaired transcriptomic homeostasis in SC-specific *Upf2* knockout testes, characterized by an accumulation of PTC-containing transcripts and the transcriptome-wide dysregulation of genes encoding splicing factors and key proteins essential for SC fate control. Our data demonstrate an essential role of UPF2-mediated NMD in prepubertal SC development and male fertility.

KEY WORDS: Nonsense-mediated mRNA decay, Premature termination codon, Alternative splicing, Sertoli cell, 3′UTR shortening, Testis, Gonocyte, Spermatogenesis, Sterility, RNA-Seq, Mouse

INTRODUCTION

Sertoli cells (SCs) are required not only for male-specific sexual differentiation during embryonic development, but also for the initiation and maintenance of spermatogenesis in postnatal development and in adulthood in mammals (Bellvé, 1998; Griswold, 1998; Cool et al., 2012). SCs originate from the epithelial cells of the genital ridges (i.e. primordial gonads), in which a subpopulation of pre-Sertoli precursor cells is determined by activation of the male sex-determining region of the Y chromosome (*Sry*) gene, which subsequently triggers a cascade of events, including the upregulation of several sex-determining factors (e.g. *Sox9*) (Morais da Silva et al., 1996; Sekido and Lovell-Badge, 2008; Larney et al., 2014). Highly proliferative primordial germ cells (PGCs) are progressively rearranged and ultimately embraced by the neighboring SCs, forming the male-specific vascularization of the testis cord by about embryonic day (E) 12.5 in mice (Fig. 1A) (Hiramatsu et al., 2009; Kashimada and Koopman, 2010; Manuylov et al., 2011; Nel-Themaat et al., 2011; Cool et al., 2012; Hu et al., 2013; Svingen and Koopman, 2013). During subsequent testis cord development, both SCs and PGCs actively proliferate (Bellvé, 1998; Svingen and Koopman, 2013). By ~E14.5-16.5, while SC proliferation continues (Cool et al., 2012), PGCs differentiate into prospermatogonia, which subsequently enter cell cycle arrest at G1 phase and remain quiescent until postnatal day (P) 3 (Culty, 2009; Moreno et al., 2010) (Fig. 1A). During postnatal testicular development, SCs continue to proliferate and the number of SCs located along the basal membrane of the testis cord increases until ~P10-15, when SCs gradually cease proliferation and undergo terminal differentiation to mature into adult SCs (Vergouwen et al., 1991; Sharpe et al., 2003). Meanwhile, prospermatogonia resume proliferation at ~P4 and differentiate into spermatogonial stem cells (A-single, A-pair and A-aligned) and more advanced progenitor spermatogonia including type A1-4, intermediate and type B spermatogonia during prepubertal testicular development. Type B spermatogonia then enter meiosis by ~P10 and sequentially become leptotene, zygotene, pachytene and diplotene spermatocytes, followed by two consecutive cell divisions to become haploid spermatids by ~P20 (McLean et al., 2003; Oatley and Brinster, 2008). It is generally believed that testis size is determined by the total number of SCs because the ratio of SCs to germ cells appears to vary among different species, but is fairly constant within the same species (e.g. 1:20 to 1:30 in mice) (Sharpe et al., 2003). Therefore, normal proliferative activities of SCs during fetal and postnatal development and the timely switch from proliferation to differentiation at ~P10-15 are all crucial for normal testicular development. Although the importance of SCs in supporting sexual differentiation, testis cord formation and development, initiation and maintenance of spermatogenesis has been broadly investigated, the intrinsic factors that control SC specification, proliferation, differentiation and maturation remain largely unknown.

Transcriptome-wide survey has revealed that ~30% of all disease-associated genetic changes, including nonsense or frameshift mutations, generate mRNA transcripts that contain premature termination codons (PTCs), and these transcripts can produce truncated proteins that are usually deleterious to cellular homeostasis (Bhuvanagiri et al., 2010; Kervestin and Jacobson, 2012; Schweingruber et al., 2013). As a RNA surveillance mechanism, the nonsense-mediated mRNA decay (NMD) machinery selectively degrades the PTC-containing (PTC[+])

[1]Department of Physiology and Cell Biology, University of Nevada School of Medicine, 1664 North Virginia Street, MS575, Reno, NV 89557, USA. [2]The Finsen Laboratory, Rigshospitalet, Faculty of Health Sciences, University of Copenhagen, Jagtvej 124, Copenhagen, DK-2200, Denmark. [3]Biotech Research and Innovation Centre (BRIC), University of Copenhagen, Jagtvej 124, Copenhagen, DK-2200, Denmark. [4]Danish Stem Cell Centre (DanStem), Faculty of Health Sciences, University of Copenhagen, Ole Maaløes Vej 5, Copenhagen N DK2200, Denmark.
*Present address: University of Texas, M.D. Anderson Cancer Center, Department of Epigenetics and Molecular Carcinogenesis, 1808 Park Road 1C, Smithville, TX 78957, USA.

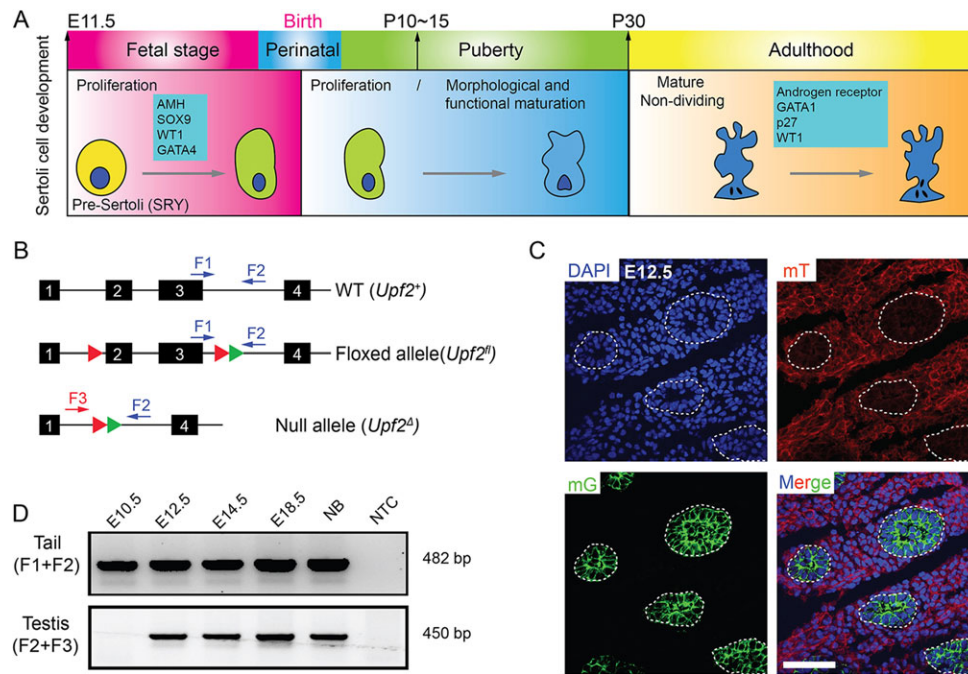‡Authors for correspondence (JianqiangBao@gmail.com; wyan@medicine.nevada.edu)

DEVELOPMENT

Fig. 1 . Generation of Sertoli cell-specific *Upf2* cKO mice. (A) Timeline of key developmental stages of murine Sertoli cells (SCs). (B) Structures of the floxed (*Upf2^fl*) and null (*Upf2^Δ*) *Upf2* alleles after Cre-mediated recombination. Arrows indicate the positions of primer pairs used for genotyping. Red triangles represent loxP cassettes and green triangles depict FRT sites. Exons are numbered. (C) Cre activities represented by specific membrane-tagged eGFP (mG) signals were detected exclusively in SCs in *Amh-Cre;Rosa26mTmG^+/tg* males at E12.5, whereas membrane-tagged Tomato red (mT) fluorescence was constitutively expressed in all cell types. Three individual mice were analyzed and representative confocal microscopy images are shown. Boundaries of the testis cords are outlined. Scale bar: 60 µm. (D) Genomic DNA PCR analyses showing Cre-mediated excision of exons 2-3 from E12.5 onwards. Sizes of PCR products (see B for primers) are as follows: F1/F2 primer pair: WT, 391 bp and floxed, 482 bp; F2/F3 primer pair: null/delete, 450 bp. NB, newborn; NTC, non-template control.

transcripts and thus plays an essential role in safeguarding the transcriptomic fidelity of the cell (Kervestin and Jacobson, 2012). The NMD machinery involves three core factors, namely UPF1, UPF2 and UPF3, which are highly conserved in eukaryotes (Schweingruber et al., 2013). NMD is triggered by recruitment of UPF1 to the ribosome stalled at the PTC position of an mRNA transcript, and the stalled ribosome subsequently recruits multiple effector factors including SMG1, SMG9, SMG8, eRF1 (ETF1) and eRF3, forming the SURF macrocomplex (Chamieh et al., 2008; Kervestin and Jacobson, 2012; Schweingruber et al., 2013). UPF2 serves as an essential scaffold, bridging the interaction between SURF and UPF3A/B deposited in the downstream exon-exon junction complex. Once the UPF1/SURF-UPF2-UPF3A/B complex is built, SMG1 kinase will quickly phosphorylate UPF1 so that numerous decay effectors, including exo- and endonucleotic decay factors, can be recruited to degrade the targets, i.e. PTC⁺ transcripts (Chamieh et al., 2008; Chakrabarti et al., 2011; Schweingruber et al., 2013).

The mechanistic details of NMD in maintaining normal transcriptomic homeostasis were largely established based on data from *in vitro* (e.g. cell culture-based) studies. Physiological evidence based on *in vivo* studies demonstrating an essential role of the NMD machinery in development has only started to emerge in recent years (Weischenfeldt et al., 2008, 2012; Thoren et al., 2010; Nguyen et al., 2013). The phenotypes observed in NMD mutants are relatively conserved among *Drosophila*, zebrafish and vertebrates. For example, UPF1, UPF2, SMG5, SMG6 and SMG7 are all essential for embryogenesis based on knockout or siRNA-mediated knockdown studies (Weischenfeldt et al., 2008; Wittkopp et al., 2009; Avery et al., 2011; Nguyen et al., 2013). In humans, mutations in *UPF1* increase the predisposition to pancreatic

adenosquamous carcinoma (ASC) due to failure in eliminating UPF1 substrate mRNAs (Liu et al., 2014), while mutations in *UPF3B* are associated with syndromic and nonsyndromic mental retardation (Tarpey et al., 2007).

Global knockout of *Upf2* leads to an early lethality phenotype before ∼E9.5 in mice, precluding further investigation of *Upf2* function in fetal and postnatal development (Weischenfeldt et al., 2008). To explore whether the NMD machinery plays a role in SC development, we inactivated *Upf2* specifically in SCs at ∼E12.5 using the Cre-loxP strategy. Here, we report that *Upf2* is required for prepubertal SC development and male fertility by controlling the fidelity of the SC transcriptome.

RESULTS

Generation of SC-specific *Upf2* conditional knockout mice

We generated SC-specific conditional knockout (cKO) mice by crossing *Upf2^fl/fl* mice (Weischenfeldt et al., 2008) with the *Amh-Cre* deletor line (Lécureuil et al., 2002). Mice of genotype *Amh-Cre;Upf2^fl/fl* are herein designated Amh-cKO, and controls refer to age-matched *Upf2^fl/fl* or wild-type (WT) mice unless otherwise stated. Similar to endogenous *Amh*, the *Amh-Cre* transgene has been reported to start to express Cre in SCs at ∼E11.5 (Fig. 1A) (Lécureuil et al., 2002). The floxed *Upf2* allele contains loxP sites flanking exons 2-3 and Cre-mediated recombination leads to a *Upf2* null allele (Weischenfeldt et al., 2008) (Fig. 1B). To determine when *Upf2* inactivation occurs in SCs in Amh-cKO mice, we crossed *Rosa26mTmG^tg/tg* mice, which is a dual fluorescence reporter line (Muzumdar et al., 2007), with *Amh-Cre* mice. Whereas the membrane-tagged Tomato red fluorescence was constitutively expressed in all cell types, the membrane-bound GFP was exclusively detected in SCs of

Amh-Cre;Rosa26mTmG$^{+/tg}$ male mice at ∼E12.5 (Fig. 1C). PCR genotyping analyses further confirmed that the recombined *Upf2* allele (*Upf2$^{\Delta}$*) was detectable in Amh-cKO testes at ∼E12.5 (Fig. 1D). These data suggest that, in Amh-cKO male mice, the *Upf2* gene was ablated specifically in SCs at ∼E12.5.

Severe testicular atrophy and infertility in adult Amh-cKO males

During a 6-month fertility test, Amh-cKO males bred with fertility-proven WT females never produced any pups, whereas the control breeding pairs (*Upf2$^{fl/fl}$*×*Upf2$^{fl/fl}$*) yielded an average of ∼7.5 pups per litter with an interval of ∼1.25 litters per month, suggesting that Amh-cKO males are sterile. Despite a similar body size between adult Amh-cKO and WT control mice (supplementary material Fig. S1A), testis weights in Amh-cKO adult males were much reduced compared with those of controls (Fig. 2A). At P16, the testis weight of Amh-cKO mice was only ∼20% of that of WT controls, and Amh-cKO testes were even smaller at P60 than at P16, suggesting deteriorating testicular atrophy (Fig. 2A,B; supplementary material Fig. S1B). Moreover, the size and weight of cauda and caput epididymides were also significantly reduced in Amh-cKO mice as compared with WT controls (Fig. 2A,C). Histologically, whereas robust spermatogenesis was observed in WT testes, some degenerated tubules containing aberrant SC-like or germ cell-like cells were sporadically present in Amh-cKO testes at P60 (Fig. 2D). Abundant spermatozoa were present in the WT cauda epididymis, whereas that of Amh-cKO males was largely empty (Fig. 2E). Together, these data indicate that conditional ablation of *Upf2* in embryonic SCs causes severe testicular atrophy and male sterility in adulthood.

Necessity of *Upf2* in prepubertal SC development

No differences in testis weight or gross morphology were observed between WT and Amh-cKO mice before P5 (Fig. 2B). However, testis weight was much reduced in Amh-cKO compared with WT males at P9, suggesting severe cell depletion at ∼P9. Histological analyses confirmed that no morphological differences existed from birth to P5 between Amh-cKO and WT mice (Fig. 3A). However, the seminiferous tubule contents were drastically reduced at P12, and the reduction continued thereafter in Amh-cKO testes (Fig. 3A). By P16, whereas the majority of seminiferous tubules contained pachytene spermatocytes in WT testes, only a few degenerating germ cells and/or disorganized SCs were present in the seminiferous tubules of Amh-cKO mice (Fig. 3B). In P60 Amh-cKO testes, seminiferous tubules were rarely seen and those that remained contained very few cells (Fig. 3B).

Based on immunofluorescence staining of the SC marker WT1 and the germ cell marker DDX4, we quantified the number of SCs and germ cells in Amh-cKO and WT testes at birth (P0), P5, P12 and P16 (Fig. 3C). Consistent with the histological analyses, no germ cell loss was observed before P5 in Amh-cKO testes, but the germ cell number declined markedly at P12 and P16 (Fig. 3C,D). Concomitant with germ cell depletion, SCs appeared to be overproduced and aggregated as clusters within the seminiferous tubules of Amh-cKO testes at P12 (Fig. 3D), suggesting a failure in transitioning from proliferative to differentiating modes during prepubertal SC development. It is noteworthy that the histology of the seminiferous tubules in Amh-cKO testes appeared to be altered even at P5, although the germ cell number remained the same as in WT controls, suggesting that the SC malfunction
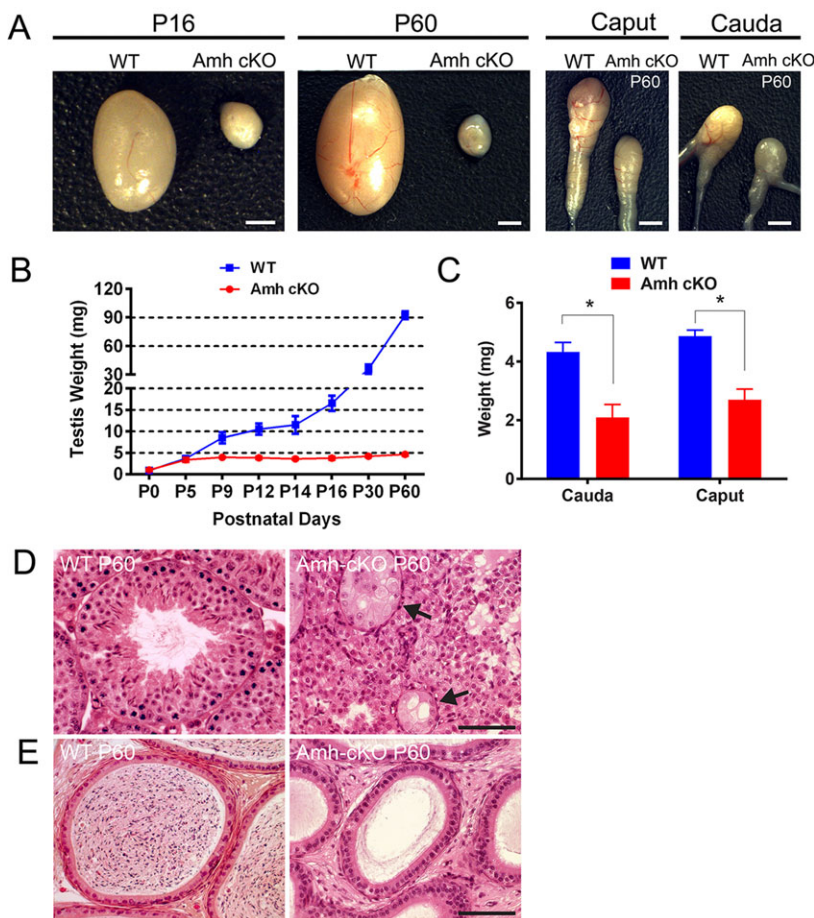

Fig. 2. Inactivation of *Upf2* in embryonic SCs leads to postnatal testicular atrophy and male sterility. (A) Gross morphology of the testis and the epididymis in WT and SC-specific *Upf2* cKO (Amh-cKO) mice at P16 and P60. (B) Testis weights in WT and Amh-cKO mice during postnatal development. Data are presented as mean±s.d. (*n*=6). (C) Weights of both caput and cauda epididymides were significantly lower in Amh-cKO mice than in WT controls at P60. Data are shown as mean±s.d. (*n*=6 per genotype). *P<0.05. (D) Histology of WT and Amh-cKO testes at P60. Full spermatogenesis was observed in the seminiferous tubules in WT testes, whereas seminiferous tubules were rare and germ cells were almost completely depleted in Amh-cKO testes. Arrows indicate germ cell-depleted tubules. (E) Histology of the cauda epididymis in WT and Amh-cKO mice. The WT cauda epididymis contained abundant mature spermatozoa, whereas no spermatozoa were present in the Amh-cKO cauda epididymis. Scale bars: 1 cm in A; 40 µm in D,E.
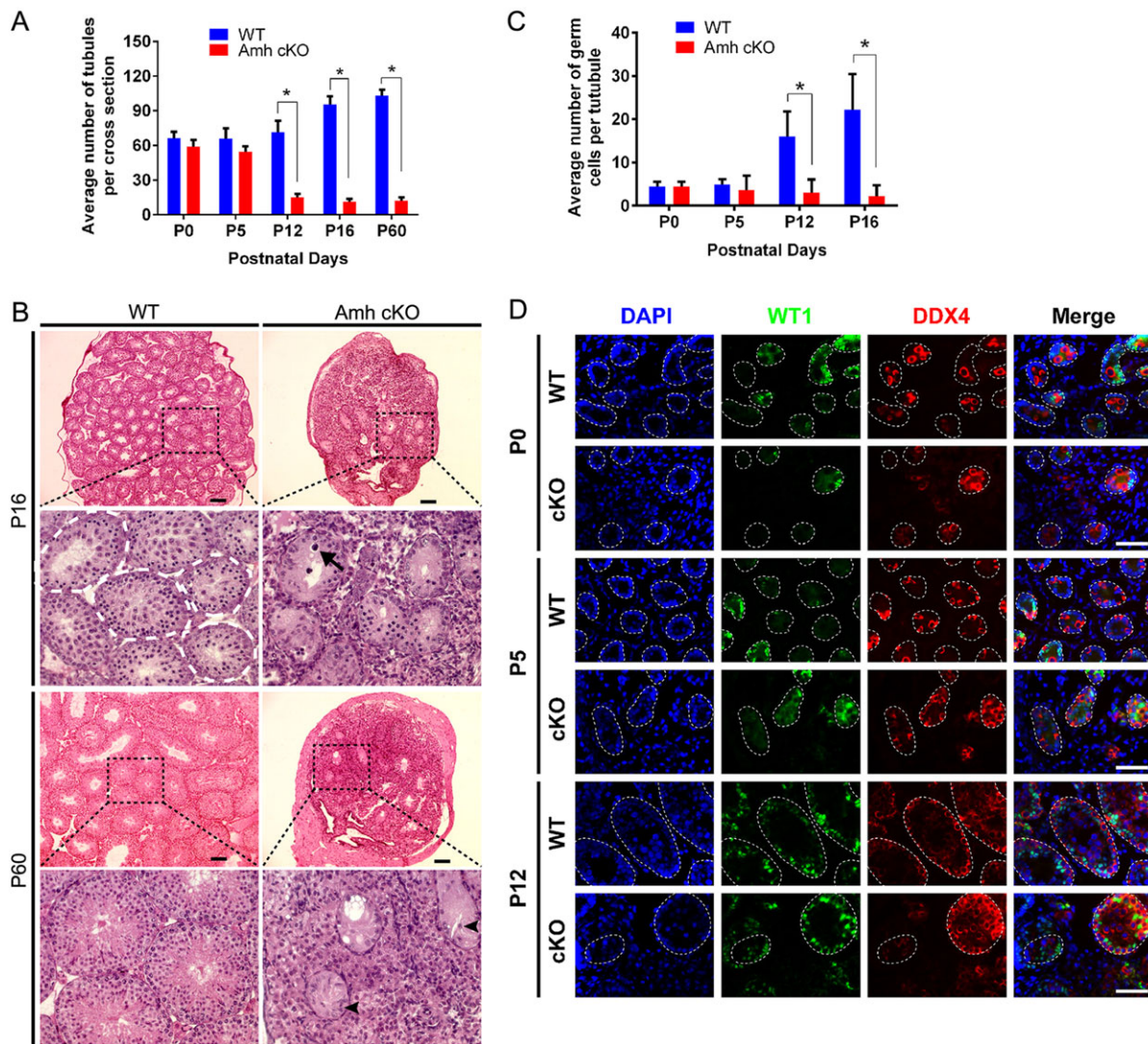
DEVELOPMENT

Fig. 3. Loss of SCs and male germ cells during postnatal testicular development in Amh-cKO mice. (A) Average number of seminiferous tubules per transverse section in WT and Amh-cKO testes at birth (P0), P5, P12, P16 and P60. At least 30 sections were scored for each of three mice per genotype at each time point, and the data are presented as mean±s.d. *$P<0.05$. (B) Histology of developing WT and Amh-cKO testes at P16 and P60. Transverse sections of WT testes contain numerous seminiferous tubules at various stages at P16 and P60, whereas only a few degenerated seminiferous tubules are present in Amh-cKO testes. The arrow points to degenerated spermatogonia-like germ cells at P16. The arrowheads indicate nuclei of disorganized SCs at P60. (C) Average number of germ cells per seminiferous tubule, counted based on immunofluorescence staining of WT1 (SC marker) and DDX4 (germ cell marker). At least 30 tubules were scored for each of three mice per genotype at each time point, and the data are presented as mean±s.d. *$P<0.05$. (D) Double immunofluorescence analyses of WT1 and DDX4 in WT and Amh-cKO testes at P0, P5 and P12. Three mice of each genotype were analyzed per time point and representative images are shown. Dashed circles delineate the boundary of each intact seminiferous tubule. Scale bars: 60 µm in B; 50 µm in D.

might have started as early as P5 (Fig. 3D). In summary, these data demonstrate that *Upf2* is required for prepubertal SC development.

Disrupted male germ cell development in Amh-cKO mice

We next investigated male germ cell development in Amh-cKO testes. By immunostaining of SOHLH1, a specific marker for prospermatogonia in fetal testes and differentiated spermatogonial populations in postnatal testes (Ballow et al., 2006), we observed no difference in the number of SOHLH1-positive progenitor spermatogonia between WT and Amh-cKO testes before P5 (Fig. 4). However, at P9, whereas spermatogonia had already begun to migrate to the basal compartment in WT testes, SOHLH1-positive germ cells in Amh-cKO testes mostly remained in the luminal compartment of the seminiferous tubules (Fig. 4). Since the

primary defects lie in SCs in Amh-cKO testes, the failure of spermatogonia to migrate to the basal compartment is likely to result from SC defects, e.g. a disrupted SC niche. Of note, in rare cases, a few morphologically spermatogonia-like germ cells were present in Amh-cKO testes at P12 and P16 (Fig. 3B,D), but were quickly eliminated, as no germ cells were present by P60. Our data suggest that *Upf2*-deficient SCs cannot support normal male germ cell development during the first wave of spermatogenesis.

Leydig cell-only appearance of older Amh-cKO testes

At the age of 3 months, both SCs and germ cells were completely absent in Amh-cKO testes (Fig. 5A,B). Seminiferous tubules were rarely seen in Amh-cKO testes at P60 (Fig. 3A) and P90 (Fig. 5A-C). Consequently, Amh-cKO testes displayed 'Leydig cell-only' histology (Fig. 5A,B). Immunostaining of CYP17, a Leydig cell
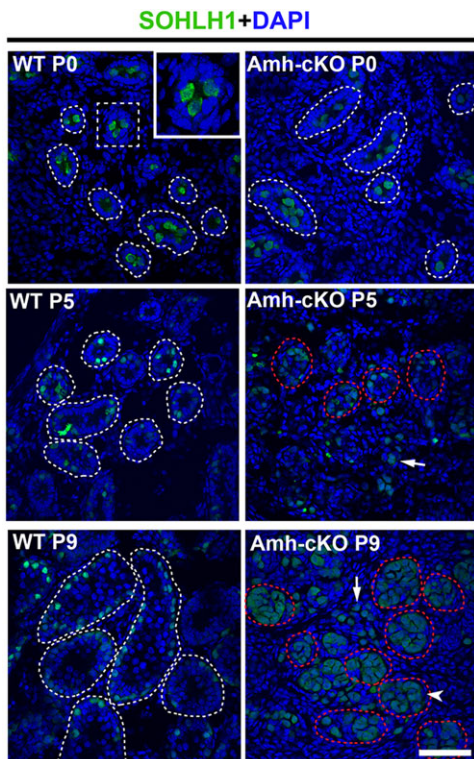
SOHLH1+DAPI

Fig. 4. Defective spermatogonial development in Amh-cKO testes.
Immunofluorescence staining of SOHLH1 (a marker for prospermatogonia and progenitor spermatogonia) in WT and Amh-cKO testes at P0, P5 and P9. The average numbers of SOHLH1-positive prospermatogonia (at P0) and progenitor spermatogonia (at P5) per tubule were comparable between WT and Amh-cKO testes. The intensity and nuclear localization of SOHLH1 were similar between WT and Amh-cKO testes. White dashed circles delineate the periphery of intact seminiferous tubules, whereas red lines encircle disorganized tubules as compared with WT. At P9, SOHLH1-positive spermatogonia are mostly situated on the basal membrane of the tubules in WT testes, whereas numerous SOHLH1-positive spermatogonia (arrowhead) appear to be aggregated randomly within the tubules in Amh-cKO testes. Arrows indicate SOHLH1-positive progenitor spermatogonia outside the disorganized seminiferous tubules. The boxed region in the WT P0 image is magnified to illustrate the area within the dashed box. Scale bar: 60 μm.

marker, revealed that the number of Leydig cells was not significantly different between WT and Amh-cKO testes at multiple time points in development (Fig. 5D). Further supporting the histological observations, qPCR analyses of multiple marker genes for SCs, Leydig cells and germ cells indicated that, despite both SCs and germ cells being drastically reduced, Leydig cells were unaffected in Amh-cKO testes (Fig. 5E). Consistently, no differences in the size and weight of the seminal vesicle, which is a testosterone-dependent reproductive organ, were observed between the WT and Amh-cKO mice (supplementary material Fig. S1B), suggesting normal testosterone production in Amh-cKO mice. Together, these data suggest that inactivation of *Upf2* in embryonic SCs impairs postnatal SC development and causes complete SC and germ cell depletion in adulthood. However, *Upf2* inactivation in SCs does not affect Leydig cell development or function.

Genome-wide disruption of the mRNA transcriptome in Amh-cKO testes

The canonical role of NMD is to maintain the fidelity of the host transcriptome by eliminating PTC$^+$ transcripts that arise from mutation, pseudogenes, retrotransposable elements or erroneous

alternative splicing (AS) events (Isken and Maquat, 2008; Kervestin and Jacobson, 2012; Schweingruber et al., 2013). We next assessed whether *Upf2* inactivation leads to genome-wide upregulation of PTC$^+$ transcripts in Amh-cKO testes. We performed RNA-Seq analyses using total testes at P4. We chose P4 because at this time point cell depletion has not started and thus the constituents in terms of the different testicular cell types are comparable between WT and Amh-cKO testes (Figs 3 and 4). More importantly, despite the lack of cell depletion at P4, the functions of SCs are highly likely to be compromised based on the altered seminiferous tubule morphology (Fig. 3D). P4 is, therefore, a unique time window for identifying mRNA transcriptomic alterations as a result of *Upf2* ablation.

Using TopHat and Cufflinks analyses (Trapnell et al., 2009), we first detected a total of 56,107 splicing transcripts in both WT and Amh-cKO testes (see GEO accession GSE58405). Among them, 1219 mRNA isoforms were significantly upregulated whereas 1373 were downregulated (cut-off: fold change ≥2, *P*<0.05) (Fig. 6A) in Amh-cKO testes at P4. Further GO enrichment analyses revealed that the upregulated transcripts were mostly involved in RNA processing, RNA splicing or cellular homeostasis (Table 1; supplementary material Table S1), suggesting that *Upf2* inactivation disrupts the RNA-processing machinery. This notion was further substantiated by the enrichment of RNA processing-related GO terms in the downregulated transcripts in Amh-cKO testes (Table 1; supplementary material Table S2). In addition, a population of transcripts related to gametogenesis was also observed in the downregulated population in Amh-cKO testes (Table 1; supplementary material Table S2). Given that germ cell development was arrested mostly at the spermatogonial stage in Amh-cKO testes (Fig. 4), these downregulated gametogenesis-specific transcripts most likely result from secondary effects, as the majority are normally expressed at a more advanced spermatogonial stage (supplementary material Table S1).

Next, we carried out PTC annotation using the spliceR pipeline (Vitting-Seerup et al., 2014). In total, spliceR detected 4545 PTC$^+$ transcripts among a total of 28,428 transcripts expressed in either WT or Amh-cKO testes [cut-off: fragments per kilobase of transcript per million mapped reads (FPKM) >1]. Among the upregulated transcripts in Amh-cKO testes, ~30% (360 out of 917) harbored PTC features, whereas this proportion declined to ~17% (227 out of 674) and ~15% (8281 out of 53,345) among the downregulated and unregulated transcripts in Amh-cKO testes, respectively (Fig. 6B). Interestingly, although some well-known NMD substrates, such as *Smg5* and *Srsf9*, were upregulated, other classical NMD targets remained unaffected in Amh-cKO testes at P4 (see GEO accession GSE58405), suggesting the target specificity of UPF2-mediated NMD in SCs. Taken together, these data suggest that there is indeed an accumulation of PTC$^+$ transcripts among those found to be upregulated in Amh-cKO testes.

Genome-wide dysregulation of splicing factors and alterations in mRNA structural features in Amh-cKO testes

It has been shown that up to 95% of human multi-exon genes generate an average of 3.5 splicing isoforms each through AS (Pan et al., 2008), and that ~30% of these splicing variants contain PTC features and thus represent a major source of PTC-interrupted transcripts. These facts suggest widespread coupling of the AS and NMD pathways (AS-NMD) (Lewis et al., 2003). Indeed, recent data have demonstrated that AS factors maintain transcriptomic homeostasis by autoregulation of their own expression at post-transcriptional levels via an NMD-mediated feedback loop (Ni et al., 2007). Therefore, we next examined whether SC-specific *Upf2*
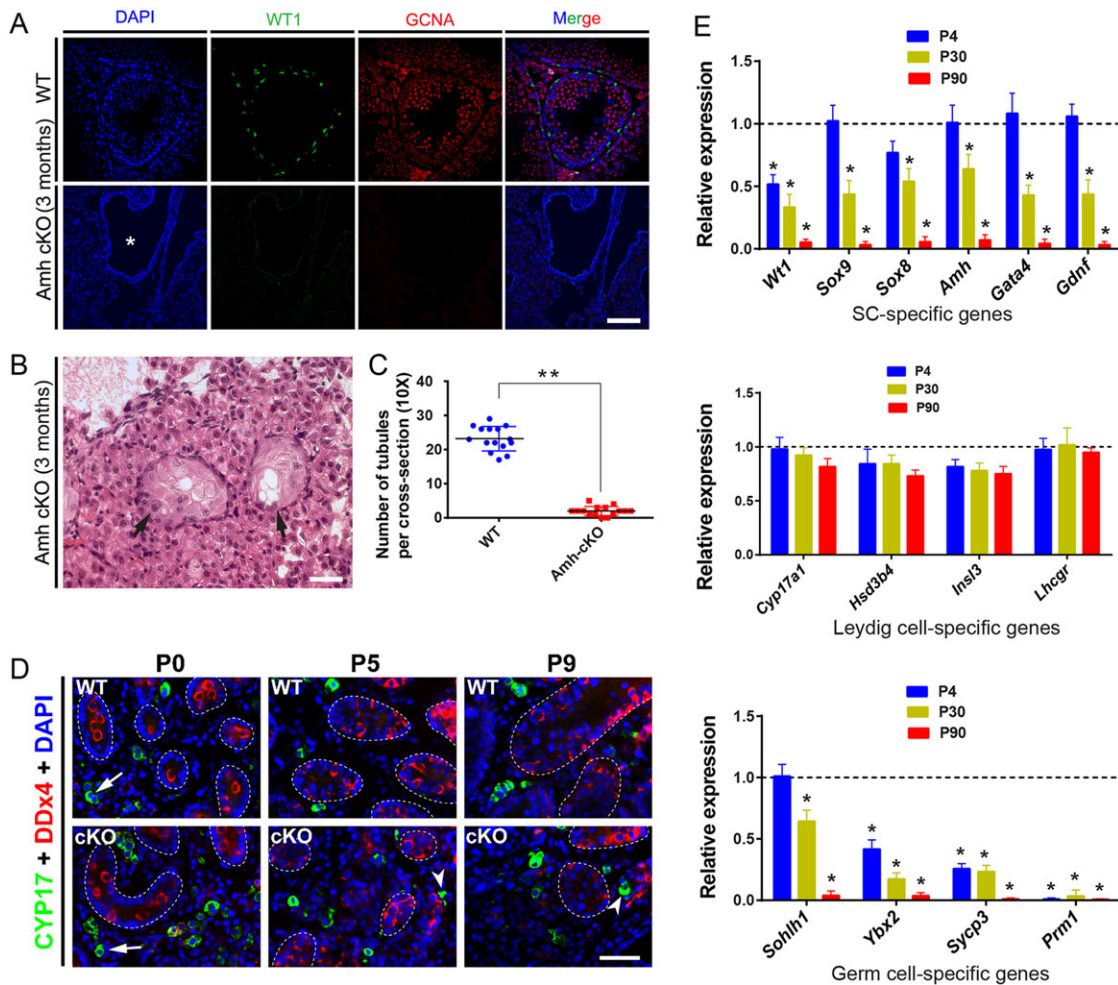
Fig. 5. Loss of seminiferous tubule architecture in Amh-cKO testes. (A) Double immunofluorescence staining of WT1 and DDX4 in 3-month-old WT and Amh-cKO testes. WT testes contain numerous seminiferous tubules with SCs situated on the basal membrane and developing male germ cells located in both basal and adluminal compartments. By contrast, SCs and germ cells are absent in Amh-cKO testes at this age. Asterisk indicates the tubules depleted of both germ cells and SCs. (B) Histology of the 3-month-old Amh-cKO testes. The residual tubules still contained a few morphologically aberrant SCs (arrows indicate nuclei). (C) Comparison of the number of seminiferous tubules per transverse section in WT and Amh-cKO testes at 3 months of age. **$P<0.01$. (D) Double immunofluorescence staining of CYP17 (a Leydig cell marker) and DDX4 (a germ cell marker) in WT and Amh-cKO testes at P0, P5 and P9. CYP17 staining is present in only a subpopulation of Leydig cells, as indicated by arrows. The average number of Leydig cells labeled by CYP17 was similar between WT and Amh-cKO testes at all three time points. Arrowheads point to germ cells within the disrupted tubules in Amh-cKO testes. (E) qPCR analysis of expression levels of mRNAs encoding marker proteins for SCs (top), Leydig cells (middle) and germ cells (bottom) in WT and Amh-cKO testes at P4, P30 and P90. For each gene at each time point, the WT expression levels were designated as 1 and the relative expression levels in Amh-cKO testes, expressed as percentage, were calculated by normalizing to WT values based on the ΔΔCt method. All data points were collected from samples in biological triplicate. *$P<0.05$. Mean±s.d. Scale bars: 50 μm.

ablation perturbs the expression levels of some of the core splicing factors in Amh-cKO testes. Indeed, RNA-Seq analyses revealed that levels of nine core splicing factors (*Hnrnpa1*, *Hnrnpc*, *Hnrnpd*, *Hnrnph1*, *Hnrnpk*, *Hnrnpl*, *Ptbp2*, *Srsf11* and *Srsf9*) were significantly downregulated or upregulated in Amh-cKO testes, as compared with WT controls (Fig. 7A). These changes were further validated by qPCR analyses, which showed similar changes in the Amh-cKO testes (Fig. 7A). In theory, dysregulated expression of core splicing factors should cause anomalies in splicing patterns genome-wide. Indeed, both the total number of AS events and the average number of AS events per transcript were higher in Amh-cKO testes than in WT controls (Fig. 7B). Of particular note, the main transcripts of *Wt1* and *Dmrt1* were significantly downregulated, and many unique, aberrant shorter transcripts were generated for both *Wt1* and *Dmrt1* in the Amh-cKO testes (supplementary material Fig. S2 and see GEO accession GSE58405). Given that both *Wt1* and *Dmrt1* are required for SC development (Raymond et al., 2000; Gao

et al., 2006; Rao et al., 2006), these changes might be responsible for the failure of SC differentiation in the absence of *Upf2*.

To reveal the genome-wide changes in the transcriptome, we performed quantitative analyses on a number of dysregulated transcripts displaying each of the eight types of splicing event, comprising exon skipping/inclusion (ESI), multiple exon skipping/inclusion (MESI), intron skipping/inclusion (ISI), alternative 5′ splicing site (A5), alternative 3′ splicing site (A3), alternative transcription start site (ATSS), alternative transcription termination site (ATTS) and mutually exclusive exons (MEE), as described previously (Vitting-Seerup et al., 2014). The total number of splicing events for ESI, A5 and A3 was much greater in the upregulated than in the downregulated transcript population in Amh-cKO testes (Fig. 7C), implying global alterations in mRNA transcript features, such as the 5′UTR, coding sequence (CDS) and 3′UTR lengths. To further test this hypothesis, we collected all transcripts that were uniquely expressed in Amh-cKO testes
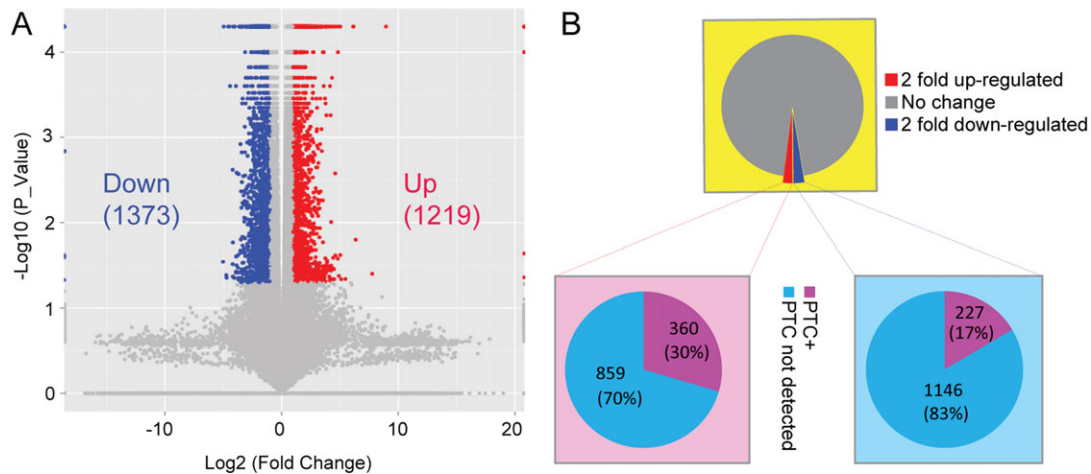
Fig. 6. Changes in the genome-wide transcriptome profile in Amh-cKO testes. (A) Volcano plot showing upregulated (red) and downregulated (blue) transcripts in Amh-cKO testes as compared with WT controls (cut-off: fold change ≥2, $P<0.05$). Among a total of 56,107 transcripts detected in both WT and Amh-cKO testes, 1219 were ≥2-fold upregulated and 1373 were ≥2-fold downregulated. (B) Premature termination codon (PTC) annotation for transcripts dysregulated in Amh-cKO testes. All transcripts detected by RNA-Seq were subjected to analysis by spliceR, an R package pipeline specifically designed for prediction of PTCs. 'Un-regulation' refers to transcripts that differed less than 2-fold between Amh-cKO and WT.

(cut-off: FPKM ≥1) and absent in WT testes (cut-off: FPKM <0.3) and compared their features with those displaying the highest expression levels (FPKM) in WT testes, since the predominant isoforms are the main contributors to the proteome (Gonzàlez-Porta et al., 2013) (Fig. 7D). Interestingly, 5′UTR and 3′UTR lengths were significantly greater in Amh-cKO than in WT testes, whereas CDS lengths were generally reduced in Amh-cKO testes (Fig. 7D).

Taken together, these data suggest that *Upf2* plays an important role in safeguarding the structural fidelity of the mRNA

Table 1. Top ranked GO terms of dysregulated genes in Amh-cKO testes ($P<0.05$)

GO terms		Gene count	P-value
Genes with ≥2-fold upregulation			
GO:0006396	RNA processing	37	5.81E–04
GO:0033554	Cellular response to stress	34	0.00112
GO:0009968	Negative regulation of signal transduction	18	2.45E–03
GO:0042592	Homeostatic process	40	1.36E–02
GO:0006468	Protein amino acid phosphorylation	42	2.19E–02
GO:0006974	Response to DNA damage stimulus	21	4.50E–02
GO:0008380	RNA splicing	16	4.67E–02
Genes with ≥2-fold downregulation			
GO:0016071	mRNA metabolic process	31	6.26E–07
GO:0048232	Male gamete generation	27	2.17E–06
GO:0045449	Regulation of transcription	121	3.06E–06
GO:0008380	RNA splicing	19	4.04E–04
GO:0022402	Cell cycle process	29	5.62E–04
GO:0006974	Response to DNA damage stimulus	23	8.36E–04
GO:0033554	Cellular response to stress	28	1.80E–03

transcriptome through, at least in part, regulating core splicing factors in developing SCs in mice.

DISCUSSION

Many genes are essential for early development and, as their inactivation leads to early embryonic lethality, this precludes further investigation of their functions in late embryonic and postnatal development. The cKO strategy overcomes this obstacle and allows for dissection of gene function in a cell lineage-specific and temporally controlled fashion. In this study, we employed an SC-specific Cre line (i.e. Amh-Cre) to inactivate *Upf2* exclusively in SCs at ~E12.5 so that the role of *Upf2* in SC development could be delineated. The dual-fluorescent reporter (*Rosa26mTmG*) line allows for easy and convenient determination of the onset of Cre activity when crossed with a specific Cre deletor line (Wu et al., 2012). Using this method, we detected Cre activity in *Amh-Cre* males at ~E12.5, which is ~2 days earlier than in an alternative *Amh-Cre* line (~E14.5) (Gao et al., 2006; Kim et al., 2010). At E12.5, SC specification has completed and the testis cord has just become morphologically distinguishable. The *Amh-Cre* line used here therefore represents a tool for inactivating a floxed gene in SCs at the earliest time point possible, i.e. E12.5.

Amh-cKO testes display no discernible differences to WT at gross and histological levels before P5, suggesting that *Upf2* is largely dispensable for fetal and perinatal SC and testicular development. However, the fact that both SCs and germ cells start to be depleted and that testis weight stops increasing after P5 indicate an arrest in prepubertal testicular development when *Upf2* is absent in developing SCs. Therefore, *Upf2* is required for prepubertal SC and testicular development. Given that inactivation of *Upf2* is confined to SCs, the primary defects must lie in the developing SCs. The onset of SC depletion at ~P10 in Amh-cKO testes coincides with the time when developing SCs normally cease proliferation and start terminal differentiation (Vergouwen et al., 1991), suggesting a cell fate control defect in *Upf2* null SCs. The timely switch from proliferative to differentiating status at ~P10-15 is crucial for establishing adult SC function, and previous studies have shown that this process requires many genes, including those encoding transcription factors [e.g. *Wt1*, *Nr5a* (*Sf1*), *Rb1*, *Wt2*, *Klf4*, *Sox8*, *Lkb* (*Stk11*), *Dmrt1* and *Aff4*], gonadotropin receptor (e.g. *Fshr*), signaling transducers (e.g. *Ctnnb1*)
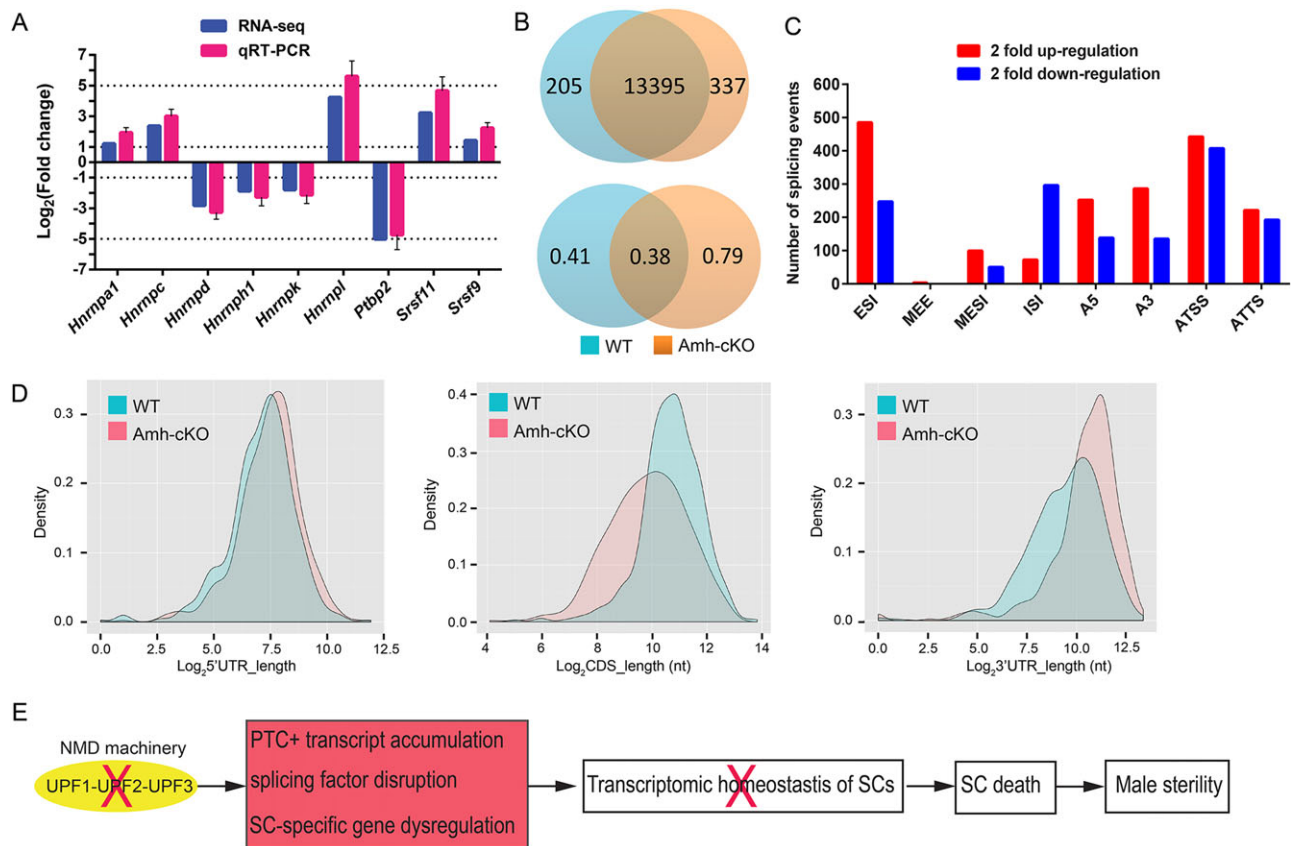
DEVELOPMENT

Fig. 7. Genome-wide alterations in mRNA splicing patterns and structural features induced by SC-specific ablation of *Upf2*. (A) Changes in mRNA levels of nine core splicing factors in Amh-cKO mice testes, as measured by both RNA-Seq and qPCR analyses. Data collected from biological triplicates are presented as mean±s.d. (B) Venn diagram showing the total number of exon skipping/inclusion events (top) and the average number of exon skipping/inclusion events per transcript (bottom) detected between WT and Amh-cKO testes. (C) Comparison of the total number of each of the eight types of splicing event detected by spliceR between 2-fold upregulated and 2-fold downregulated transcripts: ESI, exon skipping/inclusion; MESI, multiple exon skipping/inclusion; ISI, intron skipping/inclusion; A5, alternative 5′ splicing site; A3, alternative 3′ splicing site; ATSS, alternative transcription start site; ATTS, alternative transcription termination site; MEE, mutually exclusive exons. (D) Comparison of mRNA structural features, including 5′UTR length (left), CDS length (middle) and 3′UTR length (right), between WT and Amh-cKO testes at P4, as detected by spliceR. (E) Model for UPF2 functions in murine SCs. Inactivation of one of the core NMD factors, UPF2, causes disrupted transcriptomic homeostasis in SCs, characterized by accumulation of the PTC-positive transcripts, aberrant expression of splicing factors and dysregulation of SC-specific genes, which together lead to SC death and male sterility.

and small RNA biogenetic factors (e.g. *Dicer1*) (Sharpe et al., 2003; Nalam et al., 2009; Kim et al., 2010; Matson et al., 2011; Kato et al., 2012). It appears that proper cell fate control during prepubertal SC development involves the precise temporal activation of transcriptional cascades in response to hormonal stimulation (e.g. via FSH), and also the proper post-transcriptional regulation of gene expression (e.g. via miRNAs and endo-siRNAs). Our study identified *Upf2* as another essential factor that controls the crucial fate decision in developing SCs in prepubertal testes.

UPF2 is an integral component of the NMD machinery and its ablation would abolish or compromise NMD function, which would be expected to lead to an accumulation of PTC$^+$ transcripts. Indeed, PTC$^+$ transcripts account for ~30% of all upregulated mRNAs in Amh-cKO testes. In WT testes at P4, prospermatogonia have just resumed proliferative activity, and the downregulation of numerous germ cell-specific transcripts in Amh-cKO testes most likely results from germ cell defects, e.g. compromised prospermatogonial proliferation. Therefore, the PTC$^+$ transcripts should be mostly derived from the *Upf2* null SCs rather than from the germ cells, in which the NMD pathway is intact. Further evidence comes from the GO term enrichment analyses, which demonstrate that upregulated transcripts are mostly involved in RNA processing, whereas downregulated transcripts are enriched for genes relevant to

spermatogenesis (Table 1). Collectively, the accumulation of PTC$^+$ transcripts in Amh-cKO testes supports the contention that UPF2-mediated NMD plays a canonical role in developing SCs by eliminating PTC$^+$ transcripts. However, it is noteworthy that PTC$^+$ transcripts were also present at ~15-17% among both the downregulated and unregulated populations in Amh-cKO testes (Fig. 6B), suggesting the existence of an NMD-independent mechanism in post-transcriptional regulation during SC development. This notion is consistent with previous findings that NMD core factors can translocate into the nucleus and exert nuclear functions, which are often involved in biological processes other than NMD, such as cell cycle progression and the DNA stress response (Mendell et al., 2002; Brumbaugh et al., 2004; Azzalin and Lingner, 2006; Thoren et al., 2010).

Although PTC$^+$ transcripts, which account for ~30% of those upregulated in Amh-cKO testes, are considered direct targets of UPF2-mediated NMD, the remaining 70% PTC-free transcripts could also be targeted by the NMD machinery because it has been shown that certain PTC-free transcripts may contain features that trigger NMD through the non-canonical NMD pathways (Kurosaki and Maquat, 2013; Schweingruber et al., 2013). Alternatively, these upregulated PTC-free transcripts might reflect secondary effects owing to the impaired NMD machinery in the absence of UPF2. It

has been shown that splicing factors, including serine/arginine-rich (SR) proteins and heterogeneous nuclear ribonucleoproteins (hnRNPs), utilize the AS-NMD coupling mechanism to fine-tune their own levels through a negative-feedback loop (Ni et al., 2007; McGlincy and Smith, 2008; Weischenfeldt et al., 2012). Thus, the dysregulation of numerous core splicing factors observed in Amh-cKO testes is responsible, at least in part, for the genome-wide transcriptomic changes.

Recent transcriptome-wide studies in *Saccharomyces cerevisiae*, *Drosophila*, zebrafish and mammals have shown that cells deficient in NMD factors exhibit ~3-10% dysregulated transcripts, many of which are PTC free and encode full-length functional proteins (Thoren et al., 2010; Schweingruber et al., 2013). Consistently, we found that ~5% of the transcripts, comprising 1219 upregulated and 1373 downregulated among 56,107 transcripts detected, are dysregulated in Amh-cKO testes at P4. Notably, among these dysregulated genes are those encoding core splicing factors (e.g. SR proteins and hnRNPs) and those known to be essential for prepubertal SCs to switch from proliferation to differentiation at ~P10, such as *Wt1*, *Sox8* and *Dicer1* (Gao et al., 2006; Barrionuevo and Scherer, 2010; Kim et al., 2010). Therefore, the NMD pathway, in addition to its canonical function in reducing transcriptional noise, also appears to be involved in the control of expression of a subset of genes crucial for SC development.

Multiple reports have demonstrated that UPF1 can sense 3′UTR length and selectively cause degradation of mRNA transcripts with abnormally long 3′UTRs via the NMD pathway (Bühler et al., 2006; Hogg and Goff, 2010; Kurosaki and Maquat, 2013; Schweingruber et al., 2013). Consistent with these reports, our bioinformatics analyses identified numerous newly synthesized, unique transcripts with longer 3′UTRs in Amh-cKO testes (Fig. 7D), further supporting the notion that transcripts with longer 3′UTRs are more susceptible to NMD degradation. However, the accumulation of transcripts with longer 5′UTRs and/or shorter ORF in Amh-cKO testes might imply that UPF2 participates in the regulation of all three aspects of mRNA structure: 5′UTR, CDS and 3′UTR lengths.

Based on the phenotype and transcriptomic changes, including mRNA levels and structural features, induced by *Upf2* ablation in SCs, we propose that UPF2 plays an essential role by controlling the fidelity of the transcriptome in developing SCs in prepubertal testes (Fig. 7E). In brief, the UPF2-mediated NMD machinery ensures transcriptomic fidelity in prepubertal SCs by: (1) eliminating PTC$^+$ transcripts through the canonical NMD pathway; (2) regulating AS by coordinating expression levels of core splicing factors; and (3) controlling the expression of key genes essential for SC fate control during prepubertal testicular development (Fig. 7E). *Upf2* ablation causes impaired homeostasis of the SC transcriptome, as characterized by the accumulation of PTC$^+$ and erroneously spliced transcripts, and dysregulation of genes crucial for SC development, which, in turn, are manifested as severe testicular atrophy and male sterility due to failure in SC fate control and the complete demise of all SCs and germ cells. Thus, UPF2-mediated NMD represents a mechanism that is essential for prepubertal testicular development and male fertility by safeguarding the 'fitness' of the mRNA transcriptome in developing SCs.

MATERIALS AND METHODS
Animals
The Institutional Animal Care and Use Committee (IACUC) of the University of Nevada, Reno, approved all animal use protocols. Mice were housed in the pathogen-free animal facility of University of Nevada, Reno, and all mice involved in this study were on the C57BL/6J background.

Floxed *Upf2* transgenic mice (*Upf2$^{fl/fl}$*) were generated as described previously (Weischenfeldt et al., 2008). The *Amh-Cre* deletor mice were generated by Dr Guillou's laboratory (Lécureuil et al., 2002) and backcrossed onto the C57BL/6J background. The *Rosa26mTmG$^{tg/tg}$* transgenic line [strain name *Gt(ROSA)26Sor$^{tm4(ACTB-tdTomato,-EGFP)Luo}$/J*] was purchased from Jax Laboratory. Male *Amh-Cre* mice were crossed with female *Rosa26mTmG$^{tg/tg}$* mice to generate *Amh-Cre;Rosa26mTmG$^{+/tg}$* for analyzing the onset of Cre activity. To obtain *Amh-Cre;Upf2$^{fl/fl}$* (Amh-cKO) male mice, *Amh-Cre* males were crossed with *Upf2$^{fl/fl}$* females initially and the F1 heterozygotes (*Amh-Cre;Upf2$^{+/fl}$*) were then bred with *Upf2$^{fl/fl}$* to generate *Amh-Cre;Upf2$^{fl/fl}$* males.

Histology
Testes were dissected from mice at different ages followed by fixation in Bouin's solution for at least 8 h. Following dehydration through an ethanol series, the fixed testes were embedded into paraffin. Paraffin sections (5 μm) were subjected to a standard Hematoxylin and Eosin staining protocol using an automated histology station (Leica Autostainer XL Staining System ST5010) as described (Bao et al., 2014).

Immunofluorescence analyses
Testes were dissected and immediately fixed in 4% paraformaldehyde solution at 4°C overnight. The next day, testicular samples were washed in 10% sucrose solution three times for 1 h each and then embedded in OCT (Sakura Finetek) medium (50% OCT plus 10% sucrose). Cryosections (8 μm) were subjected to indirect immunofluorescence staining as described (Bao et al., 2014). Antibodies used were: WT1 (rabbit, 1:50; Santa Cruz, sc-192), purified anti-VASA/DDX4 (human, 1:500; BD, 560189), GCNA (rat, 1:10; a kind gift from Dr George Enders, University of Kansas Medical Center, Kansas City, KS, USA) (Enders and May, 1994), SOHLH1 (rabbit, 1:200; a kind gift from Dr Aleksandar Rajkovic, Magee-Womens Research Institute, Pittsburgh, PA, USA) (Suzuki et al., 2012) and CYP17 (rabbit, 1:100; a kind gift from Dr A. J. Conley, University of California, Davis, CA, USA) (Peterson et al., 2001).

Quantitative real-time PCR (qPCR)
RNA extraction and qPCR analyses were performed as previously described (Bao et al., 2013). All qPCR analyses were conducted using testicular samples in biological triplicate.

RNA-Seq
Two testes from each mouse at P4 were collected into individual 1.5 ml tubes containing 100 μl RNA Shield Solution (Zymo) and stored at −80°C until RNA isolation. Six testes from three P4 mice were pooled together as one biological replicate for RNA extraction following the protocol provided with the Direct-zol RNA MiniPrep Kit (Zymo). RNA-Seq was performed in biological triplicate at the Nevada Genomics Center, University of Nevada, Reno. The library was prepared using mRNAs purified from 2 μg total RNA for each sample following the manufacturer's instructions provided with the Ion Total RNA-Seq Kit v2 (Life Technologies). Libraries were barcoded and loaded onto the Ion PI v2 Chip for deep sequencing on an Ion Proton Sequencer (Life Technologies). RNA-Seq data were analyzed using TopHat and Cufflinks as described (Trapnell et al., 2010). For PTC annotation, the spliceR pipeline was utilized as described (Vitting-Seerup et al., 2014). Primer sequences are listed in supplementary material Table S3. RNA-Seq data are available at GEO under accession number GSE58405.

Bioinformatics analysis
Raw sequences were checked for quality using the FASTQC tool (Babraham Bioinformatics, http://www.bioinformatics.bbsrc.ac.uk/projects/fastqc/). Ends were trimmed with fastx_trimmer (purified cell populations: f=10, l=78; total testis: wt, f=11 and Stra8-KO, f=12) and then the fastq_quality_trimmer was used with parameter t=30. The resulting trimmed sequences were mapped with TopHat v2.0.9 (Trapnell et al., 2009) (default settings plus --b2-very-sensitive, -r 200 and --mate-std-dev to 100) (Trapnell et al., 2009), using mus musculus (UCSC version mm9) as reference transcriptome (provided through Illumina iGenome). Mapped RNA-Seq data were assembled with Cufflinks

v2.1.1 (Trapnell et al., 2010) (default settings plus –frag-bias-correct, –max-bundle-length 1e7, and –multi-read-correct) using mus musculus (UCSC version mm9), as well as a mask GTF file containing noncoding and other auxiliary RNA species (rRNA, misc_RNA, scRNA_pseudogene, snoRNA, snRNA, miRNA, TR_C_gene, tRNA, and mitochondrial RNA). A false discovery rate (FDR) <0.05 was required for calling differential expression between WT and KO for genes and transcripts unless otherwise stated. The resulting full-length transcripts were annotated with coding potential and classes of AS using the Bioconductor package spliceR (Vitting-Seerup et al., 2014) with default settings. Briefly, spliceR annotated transcripts with the most upstream compatible coding sequence (CDS), translated the downstream open reading frame (ORF) and outputted transcript features, including positions and lengths of ORF, 5′UTR and 3′UTR.

Statistics

Data from experiments carried out in biological triplicate were analyzed for biological significance using Student's *t*-test unless otherwise stated. $P<0.05$ was considered statistically significant.

Supplementary material
Supplementary material available online at
http://dev.biologists.org/lookup/suppl/doi:10.1242/dev.115642/-/DC1

References
Avery, P., Vicente-Crespo, M., Francis, D., Nashchekina, O., Alonso, C. R. and Palacios, I. M. (2011). Drosophila Upf1 and Upf2 loss of function inhibits cell growth and causes animal death in a Upf3-independent manner. *RNA* **17**, 624-638.

Azzalin, C. M. and Lingner, J. (2006). The human RNA surveillance factor UPF1 is required for S phase progression and genome stability. *Curr. Biol.* **16**, 433-439.

Ballow, D., Meistrich, M. L., Matzuk, M. and Rajkovic, A. (2006). Sohlh1 is essential for spermatogonial differentiation. *Dev. Biol.* **294**, 161-167.

Bao, J., Wu, J., Schuster, A. S., Hennig, G. W. and Yan, W. (2013). Expression profiling reveals developmentally regulated lncRNA repertoire in the mouse male germline. *Biol. Reprod.* **89**, 107.

Bao, J., Zhang, Y., Schuster, A. S., Ortogero, N., Nilsson, E. E., Skinner, M. K. and Yan, W. (2014). Conditional inactivation of Miwi2 reveals that MIWI2 is only essential for prospermatogonial development in mice. *Cell Death Differ.* **21**, 783-796.

Barrionuevo, F. and Scherer, G. (2010). SOX E genes: SOX9 and SOX8 in mammalian testis development. *Int. J. Biochem. Cell Biol.* **42**, 433-436.

Bellvé, A. R. (1998). Introduction: the male germ cell; origin, migration, proliferation and differentiation. *Semin. Cell Dev. Biol.* **9**, 379-391.

Bhuvanagiri, M., Schlitter, A. M., Hentze, M. W. and Kulozik, A. E. (2010). NMD: RNA biology meets human genetic medicine. *Biochem. J.* **430**, 365-377.

Brumbaugh, K. M., Otterness, D. M., Geisen, C., Oliveira, V., Brognard, J., Li, X., Lejeune, F., Tibbetts, R. S., Maquat, L. E. and Abraham, R. T. (2004). The mRNA surveillance protein hSMG-1 functions in genotoxic stress response pathways in mammalian cells. *Mol. Cell* **14**, 585-598.

Bühler, M., Steiner, S., Mohn, F., Paillusson, A. and Mühlemann, O. (2006). EJC-independent degradation of nonsense immunoglobulin-mu mRNA depends on 3′ UTR length. *Nat. Struct. Mol. Biol.* **13**, 462-464.

Chakrabarti, S., Jayachandran, U., Bonneau, F., Fiorini, F., Basquin, C., Domcke, S., Le Hir, H. and Conti, E. (2011). Molecular mechanisms for the RNA-dependent ATPase activity of Upf1 and its regulation by Upf2. *Mol. Cell* **41**, 693-703.

Chamieh, H., Ballut, L., Bonneau, F. and Le Hir, H. (2008). NMD factors UPF2 and UPF3 bridge UPF1 to the exon junction complex and stimulate its RNA helicase activity. *Nat. Struct. Mol. Biol.* **15**, 85-93.

Cool, J., DeFalco, T. and Capel, B. (2012). Testis formation in the fetal mouse: dynamic and complex de novo tubulogenesis. *Wiley Interdiscip. Rev. Dev. Biol.* **1**, 847-859.

Culty, M. (2009). Gonocytes, the forgotten cells of the germ cell lineage. *Birth Defects Res. C Embryo Today* **87**, 1-26.

Enders, G. C. and May, J. J., II. (1994). Developmentally regulated expression of a mouse germ cell nuclear antigen examined from embryonic day 11 to adult in male and female mice. *Dev. Biol.* **163**, 331-340.

Gao, F., Maiti, S., Alam, N., Zhang, Z., Deng, J. M., Behringer, R. R., Lecureuil, C., Guillou, F. and Huff, V. (2006). The Wilms tumor gene, Wt1, is required for Sox9 expression and maintenance of tubular architecture in the developing testis. *Proc. Natl. Acad. Sci. USA* **103**, 11987-11992.

Gonzàlez-Porta, M., Frankish, A., Rung, J., Harrow, J. and Brazma, A. (2013). Transcriptome analysis of human tissues and cell lines reveals one dominant transcript per gene. *Genome Biol.* **14**, R70.

Griswold, M. D. (1998). The central role of Sertoli cells in spermatogenesis. *Semin. Cell Dev. Biol.* **9**, 411-416.

Hiramatsu, R., Matoba, S., Kanai-Azuma, M., Tsunekawa, N., Katoh-Fukui, Y., Kurohmaru, M., Morohashi, K.-i., Wilhelm, D., Koopman, P. and Kanai, Y. (2009). A critical time window of Sry action in gonadal sex determination in mice. *Development* **136**, 129-138.

Hogg, J. R. and Goff, S. P. (2010). Upf1 senses 3′UTR length to potentiate mRNA decay. *Cell* **143**, 379-389.

Hu, Y.-C., Okumura, L. M. and Page, D. C. (2013). Gata4 is required for formation of the genital ridge in mice. *PLoS Genet.* **9**, e1003629.

Isken, O. and Maquat, L. E. (2008). The multiple lives of NMD factors: balancing roles in gene and genome regulation. *Nat. Rev. Genet.* **9**, 699-712.

Kashimada, K. and Koopman, P. (2010). Sry: the master switch in mammalian sex determination. *Development* **137**, 3921-3930.

Kato, T., Esaki, M., Matsuzawa, A. and Ikeda, Y. (2012). NR5A1 is required for functional maturation of Sertoli cells during postnatal development. *Reproduction* **143**, 663-672.

Kervestin, S. and Jacobson, A. (2012). NMD: a multifaceted response to premature translational termination. *Nat. Rev. Mol. Cell Biol.* **13**, 700-712.

Kim, G.-J., Georg, I., Scherthan, H., Merkenschlager, M., Guillou, F., Scherer, G. and Barrionuevo, F. (2010). Dicer is required for Sertoli cell function and survival. *Int. J. Dev. Biol.* **54**, 867-875.

Kurosaki, T. and Maquat, L. E. (2013). Rules that govern UPF1 binding to mRNA 3′ UTRs. *Proc. Natl. Acad. Sci. USA* **110**, 3357-3362.

Larney, C., Bailey, T. L. and Koopman, P. (2014). Switching on sex: transcriptional regulation of the testis-determining gene Sry. *Development* **141**, 2195-2205.

Lécureuil, C., Fontaine, I., Crepieux, P. and Guillou, F. (2002). Sertoli and granulosa cell-specific Cre recombinase activity in transgenic mice. *Genesis* **33**, 114-118.

Lewis, B. P., Green, R. E. and Brenner, S. E. (2003). Evidence for the widespread coupling of alternative splicing and nonsense-mediated mRNA decay in humans. *Proc. Natl. Acad. Sci. USA* **100**, 189-192.

Liu, C., Karam, R., Zhou, Y., Su, F., Ji, Y., Li, G., Xu, G., Lu, L., Wang, C., Song, M. et al. (2014). The UPF1 RNA surveillance gene is commonly mutated in pancreatic adenosquamous carcinoma. *Nat. Med.* **20**, 596-598.

Manuylov, N. L., Zhou, B., Ma, Q., Fox, S. C., Pu, W. T. and Tevosian, S. G. (2011). Conditional ablation of Gata4 and Fog2 genes in mice reveals their distinct roles in mammalian sexual differentiation. *Dev. Biol.* **353**, 229-241.

Matson, C. K., Murphy, M. W., Sarver, A. L., Griswold, M. D., Bardwell, V. J. and Zarkower, D. (2011). DMRT1 prevents female reprogramming in the postnatal mammalian testis. *Nature* **476**, 101-104.

McGlincy, N. J. and Smith, C. W. J. (2008). Alternative splicing resulting in nonsense-mediated mRNA decay: what is the meaning of nonsense? *Trends Biochem. Sci.* **33**, 385-393.

McLean, D. J., Friel, P. J., Johnston, D. S. and Griswold, M. D. (2003). Characterization of spermatogonial stem cell maturation and differentiation in neonatal mice. *Biol. Reprod.* **69**, 2085-2091.

Mendell, J. T., ap Rhys, C. M. J. and Dietz, H. C. (2002). Separable roles for rent1/hUpf1 in altered splicing and decay of nonsense transcripts. *Science* **298**, 419-422.

Morais da Silva, S., Hacker, A., Harley, V., Goodfellow, P., Swain, A. and Lovell-Badge, R. (1996). Sox9 expression during gonadal development implies a conserved role for the gene in testis differentiation in mammals and birds. *Nat. Genet.* **14**, 62-68.

Moreno, S. G., Attali, M., Allemand, I., Messiaen, S., Fouchet, P., Coffigny, H., Romeo, P.-H. and Habert, R. (2010). TGFbeta signaling in male germ cells regulates gonocyte quiescence and fertility in mice. *Dev. Biol.* **342**, 74-84.

Muzumdar, M. D., Tasic, B., Miyamichi, K., Li, L. and Luo, L. (2007). A global double-fluorescent Cre reporter mouse. *Genesis* **45**, 593-605.

Nalam, R. L., Andreu-Vieyra, C., Braun, R. E., Akiyama, H. and Matzuk, M. M. (2009). Retinoblastoma protein plays multiple essential roles in the terminal differentiation of Sertoli cells. *Mol. Endocrinol.* **23**, 1900-1913.

DEVELOPMENT

Nel-Themaat, L., Jang, C.-W., Stewart, M. D., Akiyama, H., Viger, R. S. and Behringer, R. R. (2011). Sertoli cell behaviors in developing testis cords and postnatal seminiferous tubules of the mouse. *Biol. Reprod.* **84**, 342-350.

Nguyen, L. S., Wilkinson, M. F. and Gecz, J. (2014). Nonsense-mediated mRNA decay: inter-individual variability and human disease. *Neurosci. Biobehav. Rev.* **46**, 175-186.

Ni, J. Z., Grate, L., Donohue, J. P., Preston, C., Nobida, N., O'Brien, G., Shiue, L., Clark, T. A., Blume, J. E. and Ares, M., Jr. (2007). Ultraconserved elements are associated with homeostatic control of splicing regulators by alternative splicing and nonsense-mediated decay. *Genes Dev.* **21**, 708-718.

Oatley, J. M. and Brinster, R. L. (2008). Regulation of spermatogonial stem cell self-renewal in mammals. *Annu. Rev. Cell Dev. Biol.* **24**, 263-286.

Pan, Q., Shai, O., Lee, L. J., Frey, B. J. and Blencowe, B. J. (2008). Deep surveying of alternative splicing complexity in the human transcriptome by high-throughput sequencing. *Nat. Genet.* **40**, 1413-1415.

Peterson, J. K., Moran, F., Conley, A. J. and Bird, I. M. (2001). Zonal expression of endothelial nitric oxide synthase in sheep and rhesus adrenal cortex. *Endocrinology* **142**, 5351-5363.

Rao, M. K., Pham, J., Imam, J. S., MacLean, J. A., Murali, D., Furuta, Y., Sinha-Hikim, A. P. and Wilkinson, M. F. (2006). Tissue-specific RNAi reveals that WT1 expression in nurse cells controls germ cell survival and spermatogenesis. *Genes Dev.* **20**, 147-152.

Raymond, C. S., Murphy, M. W., O'Sullivan, M. G., Bardwell, V. J. and Zarkower, D. (2000). Dmrt1, a gene related to worm and fly sexual regulators, is required for mammalian testis differentiation. *Genes Dev.* **14**, 2587-2595.

Schweingruber, C., Rufener, S. C., Zünd, D., Yamashita, A. and Mühlemann, O. (2013). Nonsense-mediated mRNA decay - mechanisms of substrate mRNA recognition and degradation in mammalian cells. *Biochim. Biophys. Acta* **1829**, 612-623.

Sekido, R. and Lovell-Badge, R. (2008). Sex determination involves synergistic action of SRY and SF1 on a specific Sox9 enhancer. *Nature* **453**, 930-934.

Sharpe, R. M., McKinnell, C., Kivlin, C. and Fisher, J. S. (2003). Proliferation and functional maturation of Sertoli cells, and their relevance to disorders of testis function in adulthood. *Reproduction* **125**, 769-784.

Suzuki, H., Ahn, H. W., Chu, T., Bowden, W., Gassei, K., Orwig, K. and Rajkovic, A. (2012). SOHLH1 and SOHLH2 coordinate spermatogonial differentiation. *Dev. Biol.* **361**, 301-312.

Svingen, T. and Koopman, P. (2013). Building the mammalian testis: origins, differentiation, and assembly of the component cell populations. *Genes Dev.* **27**, 2409-2426.

Tarpey, P. S., Raymond, F. L., Nguyen, L. S., Rodriguez, J., Hackett, A., Vandeleur, L., Smith, R., Shoubridge, C., Edkins, S., Stevens, C. et al. (2007). Mutations in UPF3B, a member of the nonsense-mediated mRNA decay complex, cause syndromic and nonsyndromic mental retardation. *Nat. Genet.* **39**, 1127-1133.

Thoren, L. A., Nørgaard, G. A., Weischenfeldt, J., Waage, J., Jakobsen, J. S., Damgaard, I., Bergstrom, F. C., Blom, A. M., Borup, R., Bisgaard, H. C. et al. (2010). UPF2 is a critical regulator of liver development, function and regeneration. *PLoS ONE* **5**, e11650.

Trapnell, C., Pachter, L. and Salzberg, S. L. (2009). TopHat: discovering splice junctions with RNA-Seq. *Bioinformatics* **25**, 1105-1111.

Trapnell, C., Williams, B. A., Pertea, G., Mortazavi, A., Kwan, G., van Baren, M. J., Salzberg, S. L., Wold, B. J. and Pachter, L. (2010). Transcript assembly and quantification by RNA-Seq reveals unannotated transcripts and isoform switching during cell differentiation. *Nat. Biotechnol.* **28**, 511-515.

Vergouwen, R. P. F. A., Jacobs, S. G. P. M., Huiskamp, R., Davids, J. A. G. and de Rooij, D. G. (1991). Proliferative activity of gonocytes, Sertoli cells and interstitial cells during testicular development in mice. *J. Reprod. Fertil.* **93**, 233-243.

Vitting-Seerup, K., Porse, B. T., Sandelin, A. and Waage, J. (2014). spliceR: an R package for classification of alternative splicing and prediction of coding potential from RNA-seq data. *BMC Bioinform.* **15**, 81.

Weischenfeldt, J., Damgaard, I., Bryder, D., Theilgaard-Monch, K., Thoren, L. A., Nielsen, F. C., Jacobsen, S. E. W., Nerlov, C. and Porse, B. T. (2008). NMD is essential for hematopoietic stem and progenitor cells and for eliminating by-products of programmed DNA rearrangements. *Genes Dev.* **22**, 1381-1396.

Weischenfeldt, J., Waage, J., Tian, G., Zhao, J., Damgaard, I., Jakobsen, J. S., Kristiansen, K., Krogh, A., Wang, J. and Porse, B. T. (2012). Mammalian tissues defective in nonsense-mediated mRNA decay display highly aberrant splicing patterns. *Genome Biol.* **13**, R35.

Wittkopp, N., Huntzinger, E., Weiler, C., Sauliere, J., Schmidt, S., Sonawane, M. and Izaurralde, E. (2009). Nonsense-mediated mRNA decay effectors are essential for zebrafish embryonic development and survival. *Mol. Cell. Biol.* **29**, 3517-3528.

Wu, Q., Song, R., Ortogero, N., Zheng, H., Evanoff, R., Small, C. L., Griswold, M. D., Namekawa, S. H., Royo, H., Turner, J. M. et al. (2012). The RNase III enzyme DROSHA is essential for microRNA production and spermatogenesis. *J. Biol. Chem.* **287**, 25173-25190.

DEVELOPMENT